Ecological Modelling, 43 (1988) 155–182
Elsevier Science Publishers B.V., Amsterdam – Printed in The Netherlands

MINLAKE: A DYNAMIC LAKE WATER QUALITY SIMULATION MODEL

MICHAEL J. RILEY and HEINZ G. STEFAN

St. Anthony Falls Hydraulic Laboratory, Department of Civil and Mineral Engineering, University of Minnesota, Minneapolis, MN 55414 (U.S.A.)

(Accepted 5 April 1988)

ABSTRACT

Riley, M.J. and Stefan, H.G., 1988. MINLAKE: a dynamic lake water quality quality simulation model. *Ecol. Modelling*, 43: 155–182.

A dynamic, one-dimensional, unsteady lake water quality simulation model is described. The model is intended primarily for lake eutrophication studies and control strategies. The model attempts to simulate the continuous change of lake stratification and water quality in response to weather, inflow, outflow, exchange processes at the sediment interface and inlake processes. The latter include advective and diffusive transport, settling, chemical and biological kinetics. A Lagrangian approach is used for the simulation of transport processes. The model uses horizontal layers of time variable thickness. The water quality parameters modeled include temperature, up to three forms of algae (expressed as chlorophyll-*a*), several forms of phosphorus and nitrogen, detritus, zooplankton, inorganic suspended sediment and dissolved oxygen. The model simulates each parameter as a function of depth in 1-day timesteps. The model can be run on a personal computer.

MODEL PURPOSE

Lake eutrophication is a continuing and growing problem in many parts of the world. Many lake and watershed treatments have been developed to offset problems and to remove the causes of eutrophication. Often, methods have yielded satisfactory results on one lake, but were not effective on others. The failure of particular lake treatment methods is believed to include insufficient understanding of the contributions of nutrients from internal and external sources, and the dynamics of physical, biological and chemical interactions in a lake. Models often used to understand the processes have tended to be very general steady-state models (e.g. Dillon and Rigler, 1975; Vollenweider, 1975; Walker, 1985) or highly complex models applicable only to a specific lake (e.g. Scavia, 1980; Bierman and

0304-3800/88/$03.50

Dolan, 1981; Matsuoka et al., 1986; and Cochrane et al., 1987). Finally, many models cannot satisfactorily simulate different treatment options but were developed to test only one treatment.

The Minnesota Lake Water Quality Management Model (MINLAKE) was developed to satisfy some of the needs in shallow temperate lake management and to eliminate some of the shortcomings of earlier models. The model was developed from a model for temperature and suspended solids (Ford and Stefan, 1980; Dhamotharan et al., 1981), and an early version (RESQUAL II) has been applied to Lake Calhoun, Minn. (Gulliver and Stefan, 1982), Lake Chicot, Ark. (Stefan et al., 1982) and the Fairmont Lakes, Minn. (Hanson and Stefan, 1985). More recently, the MINLAKE model has been applied to Round Lake, Minn. (Riley and Stefan, 1986; Riley et al., 1988), and several other lakes are currently under study. Model development followed five main criteria: (1) that the model be general for use on different lakes with a minimum of alterations, (2) that the model be capable of simulating a wide range of treatment options, (3) that the model incorporate the dominant physical, chemical and biological processes in a lake, especially processes directly affected by various lake treatment options, (4) that the physical, chemical and biological components be modeled with similar orders of detail to reduce the possibility of a weak link in the modeling process, and (5) that the model be economical enough to run to serve as a management tool.

The different development criteria placed considerable constraints on the model design. The third and fourth criteria require a detailed model of chemical and biological processes while the last one favors the use of simple models. Model development focused on the selection of spatial and temporal resolution, state variables and processes without developing a model too elaborate and expensive to operate. A one-dimensional spatial resolution (vertical) and a time step of 1 day were chosen. In the one-dimensional approximation the lake is treated as a series of horizontally homogeneous layers. The thickness of the layers is variable and the upper and lower allowable layer thicknesses are chosen by the user. The one-dimensional approximation prohibite the simulation of horizontal nonhomogeneities and localized effects that may be important on large water bodies. Consequently, the model is more suitable for small lakes on the order 50–100 km^2 or less. The 1-day time step excludes the use of the model in ecological studies of diurnal and nocturnal processes.

Development of multi-dimensional, diurnal-nocturnal models is not supported by the usual availability of lake data, since most lake monitoring programs produce only daytime measurements at one location in a lake.

The availability of data and cost constraints also influenced the selection of state variables. It was decided to include commonly measured lake quality

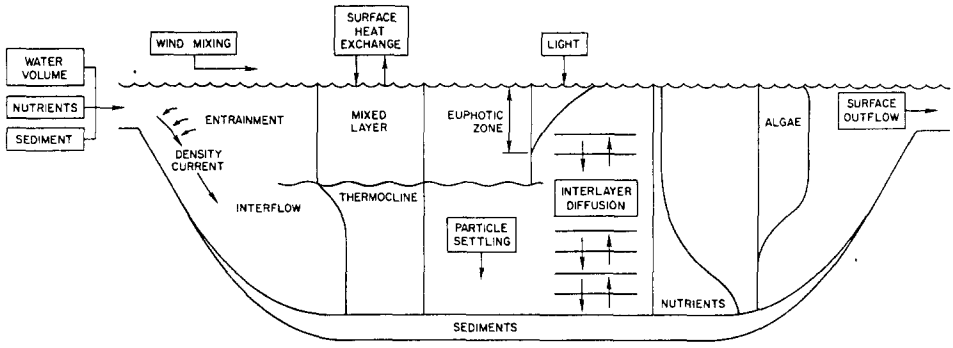

Fig. 1. Schematic diagram of the processes represented in the MINLAKE model.

parameters as state variables but not to develop complex models of nutrient dynamics. Similarly, the trophic levels explicitly represented in the model were limited to two: algae and zooplankton. Data on the time variation of fish populations are seldom available even on a monthly or seasonal basis. Therefore, the effect of fish is restricted to the selection of zooplankton predation coefficients.

Biological processes such as growth, mortality and predation are source or sink terms in the material transport equations. It was decided to limit the processes represented in the model to those processes that are directly affected by lake restoration alternatives. Consequently, some processes are not explicitly included in the model but are combined into bulk rate coefficients, e.g. of mortality, growth, etc.

The restrictions on the number of state variables and the processes represented make the model less suitable for ecological studies of inter-species interactions and species succession. The model is more specifically designed to provide an adequate representation of the interactions among algae, zooplankton and nutrients in the simulation of the effects of lake restoration strategies.

The main processes simulated by the model are illustrated in Fig. 1.

MODEL STRUCTURE

The MINLAKE program has five main sections: input, heat budget, biological-nutrient kinetics, inflow–outflow subroutines, and the lake-specific subroutine. A schematic diagram showing the information flow is given in Fig. 2.

The input section provides the information necessary to begin the computation sequence: the rate coefficients and yield coefficients used to calibrate the model to a particular lake and the meteorological data for each day of the computation period. The initial conditions and the calibration variables

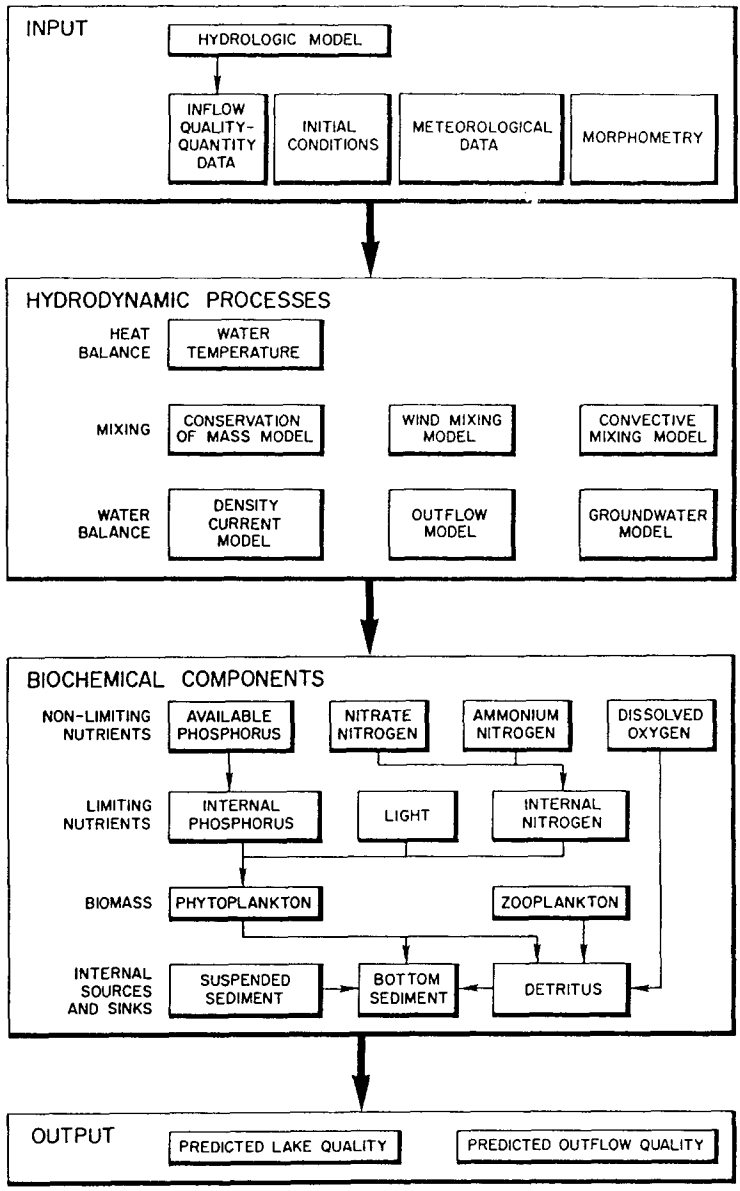

Fig. 2. Schematic diagram of information flow in the model.

are read only once while the meteorological data are accessed at the beginning of each month of simulation.

The heat budget section is the first of the modeling sequences. In it the meteorological data is used to compute the surface heat exchange, the subsurface attenuation of solar radiation, and the extent of wind mixing. The heat balance and the wind mixing determine the temperature profile

and the depth of the mixed layer. The heat budget routine also simulates natural convective mixing when the surface water cools more rapidly than water below the surface. The heat budget routine uses an integral energy approach as given by Ford and Stefan (1980).

The biological-nutrient section is the most complex part of the program. The complexity is due to the interrelationships among materials and biota in the water. The biology is characterized by one to three phytoplankton groups and one zooplankton group. The growth of the phytoplankton in the model is potentially limited by phosphorus, nitrogen as either nitrate–nitrite or ammonium, or light, all of which are used as variables. Light penetration is computed based on incoming solar radiation and attenuation of light with depth. In addition, detritus is modeled as a pool of oxygen consuming, decaying organic matter which is linked to the dissolved-oxygen concentration and releases nutrients during the decay process.

The inflow–outflow section simulates the variations in lake stage and inflow of nutrients. Inflow and outflow can be either input parameters or computed. The inflow must be specified in terms of flow rate, temperature, and the concentration of nutrients, detritus and dissolved oxygen. The input data become considerable, especially if there is more than one source of inflow. A separate hydrological model can be used to generate the inflow quantity and quality from each source based on meteorological conditions but is not provided with MINLAKE. The inflow can plunge to any layer depending on its density.

Outflow is specified only in terms of flow rate. The outflow removes a volume of water with dissolved and suspended material concentrations calculated by MINLAKE.

The lake-specific subroutine is constructed to include functions for fetch, depth–area and depth–volume relationships, inflow and outflow volume computations and additional processes for nutrient depletion or nutrient input. The lake-specific subroutine enables a user to modify the program for an application to a specific lake or simulation of a particular treatment process without modifying the existing program. The lake-specific subroutine can also be used as a link between MINLAKE and complex, multi-subroutine submodels for rainfall–runoff computations or the simulation of complex lake treatment processes such as destratification devices. The lake-specific subroutine is maintained as a separate file, is compiled separately and linked to the main program prior to operating the model.

BASIC GOVERNING EQUATIONS AND NUMERICAL SOLUTION SCHEMES

The dynamics of all substances (state variables) in a horizontal water layer whether dissolved or suspended can be expressed by the same one-di-

mensional advection–diffusion equation:

$$A\frac{\partial C}{\partial t} + v\frac{\partial (CA)}{\partial z} = \frac{\partial}{\partial z}\left(KA\frac{\partial C}{\partial z}\right) \pm \text{sources/sinks} \tag{1}$$

where C is concentration or intrinsic property of the fluid (such as heat content); v vertical settling velocity of the substance ($=0$ for dissolved substances and temperature); z vertical coordinate measured positively downward; K vertical turbulent diffusion coefficient (assumed to be identical for each state variable); and A horizontal area of the control volume. The advection–diffusion equation is applied to any one variable by the choice of source and sink terms. The sources and sinks determine the complexity of the model and the interrelationship among the variables.

The one-dimensional vertical advection–diffusion equation is discretized using a series of layers characterized by depth from the surface, thickness, layer volume, and horizontal areas at the top and through the midpoint of the layer. One of two methods of discretization is used for all variables, except temperature depending on whether or not there is a component of velocity in the vertical direction. Both solutions use a fully implicit solution for a control volume. The dissolved substances use a central difference scheme to discretize the partial differential equations. The suspended state variables (chlorophyll, suspended sediment, and detritus) are not modeled by a simple central difference scheme due to the dual effect of advection and diffusion. The discretization is taken from the suspended sediment model developed by Dhamotharan et al. (1981) and uses the implicit power-law scheme developed by Patankar (1979). Temperature simulation uses an integral energy approach that treats heat flux in, heat flux out, and wind mixing in a sequential manner (Ford and Stefan, 1980).

The discretization of each equation yields a set of linear equations, one for each layer, which are solved simultaneously. Because the concentration of a variable within a layer is only dependent on the concentration in the two adjacent layers, the set of equations is assembled into a tri-diagonal matrix. A modified Gause elimination procedure is used to solve the tri-diagonal matrix producing a fast, economical and stable solution.

SETTLING VELOCITIES AND TURBULENT DIFFUSION COEFFICIENTS

The settling velocity of algae and detritus is treated as a constant. The settling velocity of suspended sediment is taken as a function of the particle diameter and the dynamic viscosity of the layer (computed from the temperature) (Gibbs et al., 1971).

The diffusion coefficient is computed independently for each layer. The diffusion coefficient between adjacent layers is then computed as the

harmonic mean of the two values. In the surface mixed layer, the diffusion coefficient is computed as a function of wind velocity (Stefan et al., 1982):

$$K = 28W^{1.3} \tag{2}$$

where W is wind speed (MPH ≈ 1.609 km h^{-1} ≈ 0.447 m s^{-1}). The computation results in a large value for the coefficient which in turn yields a uniform profile for suspended substances in the mixed layer. In the thermocline and hypolimnion, the diffusion coefficient is computed using the Brunt–Väisälä frequency (Jassby and Powell, 1975):

$$K = 0.00866 K_{\max} N^{-1} \qquad \text{with} \quad N = \left(\frac{g}{\rho} \frac{\partial \rho}{\partial z} \right)^{1/2} \tag{3}$$

where $K_{\max}$ is maximum hypolimnetic diffusion coefficient; and N Brunt–Väisälä frequency.

The function is truncated such that the value of K does not exceed $K_{\max}$. The value of $K_{\max}$ is estimated based on the surface area of the lake (Mortimer, 1942; Jassby and Powell, 1975) and can be adjusted in calibration of the model.

PHYTOPLANKTON KINETICS

The prediction of algal biomass is the main purpose of the model and together with the nutrient routines comprises the bulk of the program. Biomass concentration can be expressed in a number of different ways including dry weight of algae, carbon content, and chlorophyll-*a* concentration. There are assumptions required to use any of the expressions for algal concentration. Use of dry weight or carbon content assumes that productivity is directly related to biomass. However, productivity is more closely related to the chlorophyll-*a* content of an algal cell. Use of chlorophyll-*a* as a measure of biomass assumes that chlorophyll is directly related to biomass. In fact, chlorophyll content can fluctuate independently of biomass to meet the phytosynthetic needs of the cell (Bannister, 1974; Schlesinger and Shuter, 1981). Because the purpose of the model is to determine productivity rather than actual biomass, the concentration of chlorophyll-*a* in a water volume is used to represent an algal population.

Fluctuations in phytoplankton populations in a volume of water are due to the combined effects of growth, diffusion, settling, respiration, and grazing. The differential equation for the time rate of change of the phytoplankton population is given in Fig. 3 as a schematic representation of each process. The solution of the equation follows the form for a variable with a settling velocity.

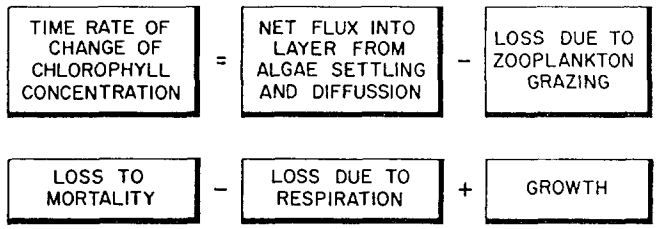

Fig. 3. Schematic representation of the differential equation for phytoplankton dynamics.

Three levels of complexity for phytoplankton modelling are provided.

(1) The first level of phytoplankton modeling uses a single algal group with productivity distributed throughout the mixed layer and euphotic zone. Forsberg and Shapiro (1981) presented a relationship for growth as a function of light, phosphorus, and mixed layer depth as:

$$R = \frac{\ln\left(\frac{I_0}{I_{z'}}\right) P_{\max}}{\epsilon_w + \epsilon_c C}\left[1 - \frac{k_{q'} C}{S_0}\right]\frac{1}{z_m Y} - D \tag{4}$$

where R is specific growth rate (day^{-1}); C concentration of chlorophyll-*a* (mg Chl.-*a* m^{-3}); I_0 intensity of photosynthetically active radiation (PAR) just below the surface; $I_{z'}$ intensity of PAR at depth z'; z' empirically defined water depth (m); $P_{\max}$ maximum specific daily rate of photosynthesis under nutrient saturated conditions (mg C (mg Chl.-*a* day)$^{-1}$; z_m mixed layer depth (m); D specific loss rate due to settling, grazing and metabolism (day^{-1}); Y carbon to chlorophyll-*a* mass ratio; ϵ_c attenuation coefficient of PAR by chlorophyll-*a* (m^2 (mg Chl.-*a*)$^{-1}$); ϵ_w attenuation coefficient of PAR by water and substances other than chlorophyll-*a* suspended and dissolved in water (m^{-1}); S_0 concentration of limiting nutrient (mg m^{-3}); and $k_{q'}$ minimum S_0/C ratio for photosynthesis to occur (cell quota).

Although the list of variables appears to be prodigious, most of the variables are known or easily determined. The term $\ln(I_0/I_{z'})$ is approximately constant at 1.9 if the incoming solar radiation exceeds 320 Ly day^{-1} which it does for most of the summer (Forsberg and Shapiro, 1981). Because $\ln(I_0/I_{z'})$ is known, z' does not have to be determined. S_0, ϵ_w, ϵ_c, Y, and z_m are either input parameters or computed by the model. D, $k_{q'}$, and $P_{\max}$ are left as calibration parameters.

The level-1 model attempts to combine all the growth and loss terms into one equation and is based on previous work by Megard et al. (1979). The chlorophyll-*a* concentration is computed directly and applied to all the layers within the mixed layer.

The level-1 model equation is subject to two specific assumptions (Forsberg and Shapiro, 1981): the phytoplankton population is assumed to be uniformly distributed throughout the mixed layer; and it is assumed that the light intensity at some point in the mixed layer reaches the level for light-saturated photosynthesis to occur. Although there is some doubt that both assumptions are satisfied each day of the simulation, the equation is adequate for the purpose of a quick and simple calculation of chlorophyll-*a* concentration.

(2) The second level of phytoplankton modeling is also a single algal group model, but the growth term is unique to each layer. The 2nd-level model represents algal growth by a Michaelis–Menten equation (Monod, 1949) subject to both light and phosphorus limitation. The Michaelis–Menten equation for growth limitation is given by:

$$\mu = \mu_{\max}\left(\frac{S}{K_s + S}\right) \tag{5}$$

where $\mu_{\max}$ is maximum (nutrient saturated) growth rate (day^{-1}); S concentration of a limiting nutrient ($mg\ l^{-1}$); and K_s half saturation concentration of nutrient ($mg\ l^{-1}$).

Phosphorus and light limitation are applied on the assumption of a single limiting factor. The effect of multiple nutrient limitation is often presented as a multiplicative effect (Lehman et al., 1975; Jørgensen et al., 1978). In fact, the effect of multiple limiting nutrients is probably neither singular nor multiplicative (Monod, 1949). However, the multiplicative method results in an extremely severe limitation of growth. In a direct comparison of limiting nutrient and multiplicative approaches, the single limiting nutrient more closely simulates the fluctuations of algal populations (De Groot, 1983) and this approach is also used here.

Light limitation is simulated by a function to describe light-limited growth and inhibition (Megard et al., 1984) using the average quantum of photosynthetically active radiation ($\mu E\ m^{-2}\ s^{-1}$) within a layer:

$$L_I = \frac{I\left(1 + 2\sqrt{K_1/K_2}\right)}{I + K_1 + I^2/K_2} \tag{6}$$

where L_I is light-limited growth ratio (between 0 and 1); I photosynthetically active irradiance ($\mu E\ m^{-2}\ s^{-1}$); and K_1, K_2 light limitation and inhibition coefficients, respectively ($\mu E\ m^{-2}\ s^{-1}$).

E, einstein = 1 mol of quanta, which is equivalent to 6.022×10^{23} photons.

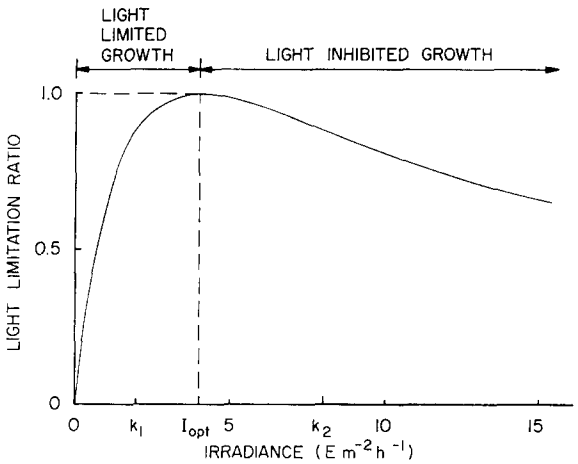

Fig. 4. Light growth and inhibition function indicating regions of light-limited growth and light-inhibited growth.

A typical form of the relationship is given in Fig. 4. The incoming solar radiation is attenuated with depth using extinction coefficients for water, chlorophyll-*a*, and suspended sediment. The conversion from energy units to quantum units is given by Combs (1977) as:

$$I_s = \frac{27.25}{\text{TD}} H_s \tag{7}$$

where I_s is average photosynthetically active radiation (PAR) over the daylight period (μE m^{-2} s^{-1}); TD photo-period (h); and H_s solar radiation (cal cm^{-2} day^{-1}).

The average quantum in a layer is found by integrating the light attenuation function over the thickness of a layer divided by the thickness (Cardoni and Stefan, 1981) and is expressed as:

$$I_{\text{ave}} = \frac{I_i\left[1 - \exp\left(-kD_{z_i}\right)\right]}{kD_{z_i}} \tag{8}$$

where I_{ave} is average PAR in layer i (μE m^{-2} s^{-1}); I_i PAR reaching the top of the layer (μE m^{-2} s^{-1}); k extinction coefficient (m^{-1}); and D_{z_i} thickness of layer i.

In the model, the light availability is calculated on eight subdivision of the photo-period and using 0.2-m sublayers within each layer.

---

cal, calorie (International Table) = 4.1868 J (def).

(3) The third level of phytoplankton modeling is more complex than the previous models. Instead of one algal group, up to three classes of algae may be utilized. By modeling the three very rough classes, the level-3 model can be used to simulate the shift from diatoms early in the season to green and then blue-green algae during the summer. The distinction between algal groups is given by different rates of photosynthesis, respiration, settling, zooplankton grazing, and different nutrient requirements.

Nutrients limitation on growth is presented as a two-step process in the 3rd level model. Growth is treated as independent of the external nutrient level, but is dependent on the available light within a layer or on the Internal nutrient content of the algal group. The growth rate is determined by the single limiting nutrient concept with limitation from internal phosphorus or light. An option is available to also treat two classes of algae as limited by internal nitrogen. The growth limitation by internal nutrients is described by Lehman et al. (1975) and Jørgensen et al. (1978):

$$\mu = \mu_{\max} \frac{N - (\text{Chl.-}a)(N_{\min})}{N} \tag{9}$$

where $\mu_{\max}$ is nutrient saturated growth rate (day^{-1}); N internal nutrient concentration (mg l^{-1}); Chl.-a concentration of chlorophyll-a (mg l^{-1}); and $N_{\min}$ minimum ratio of phosphorus to chlorophyll-a. The minimum phosphorus/chlorophyll-a ratio is estimated stoichiometrically using phosphorus/carbon ratios (Stumm and Morgan, 1981) and assuming a constant carbon/chlorophyll-a ratio of 50. The actual carbon chlorophyll ratio may vary from 25 to 100 (Schlesinger and Schuter, 1981), depending on the light adaptation and the physical condition of the algae; the lowest ratios are found in low light adapted algae and higher ratios in highly stresses algae. By setting a constant minimum phosphorus/chlorophyll-a ratio, some inaccuracy is introduced at low-light levels where growth will be light-limited.

The internal nutrient pool is modeled in much the same way as chlorophyll. Respiration, mortality, settling, and grazing reduce the concentration of internal nutrient stores. The internal nutrient concentration is increased through nutrient uptake from the water. The rate of uptake is affected by both the initial internal nutrient concentration and by the concentration of the nutrient in the water. The uptake relationship is given by Lehman et al. (1975) and Jørgensen et al. (1978) as:

$$u = u_{\max} \frac{(\text{Chl.-}a)(N_{\max}) - N}{(\text{Chl.-}a)(N_{\max} - N_{\min})} \frac{S}{K_s + S} \tag{10}$$

where $u_{\max}$ is maximum uptake rate (day^{-1}); $N_{\max}$ maximum ratio of nutrient to chlorophyll-a; $N_{\min}$ minimum ratio of nutrient to chlorophyll-a; Chl.-a chlorophyll-a concentration (mg l^{-1}); S nutrient concentration in the

water (mg l^{-1}); K_s half-saturation constant for uptake (mg l^{-1}); and N internal nutrient concentration (mg l^{-1}).

The first ratio in the equation represents a decrease in the maximum uptake rate due to the nutrient deficit within the algal population. The second ratio is a decrease in the rate of nutrient uptake due to the nutrient concentration in the water.

In most phytoplankton models, the growth rate is related only to the external nutrient concentration as in the second level model discussed earlier (DiToro and Connolly, 1980; Scavia, 1980; Walters, 1980). The assumption is made that internal nutrient content of the phytoplankton is always in equilibrium with the nutrient concentration in the water column. The assumption is based on the high rate of uptake relative to the growth rate (DiToro, 1980). The assumption is valid for the case of an increasing nutrient concentration where the rapid uptake causes the increased growth rate to be well correlated with the increased nutrient concentration. The equilibrium approach must notably breaks down under nutrient depletion where growth continues despite the low nutrient content of the water due to the internal abundance of nutrients.

The internal nutrient concept has been used in a number of models (Lehman et al., 1975; Jørgensen et al., 1978). The previous models have been zero dimensional models treating the entire lake as a well mixed body. Use of the internal nutrient concept in a single-dimension model in depth causes some problems in the mixing of phytoplankton of different internal nutrient content from different layers due to settling and diffusion. Ideally, the model would track individual cells in diffusion, settling, uptake, and growth (cell division). This, of course, is not practical.

The alternative used in the present model treats all the phytoplankton of one algal group within a layer as having the same internal nutrient content. Consequently, the solution of the equations conserves mass, but moderates the growth rate and uptake rate by essentially averaging the internal nutrient content of algae transferred into a layer with the algae already in a layer. The non-linear relationship between internal nutrients and growth is marked by two approximately linear ranges and a non-linear range. The effect of averaging the internal nutrient content will only introduce an error in the non-linear portion of the curve. The magnitude of the error will depend on the difference between the internal nutrient content in adjacent layers. In the mixed layer where most of the growth will occur, the internal nutrient content does not vary much between layers and the effect on growth is minimal.

The growth rates of all phytoplankton populations are also affected by the water temperature. Different functions developed to represent the temperature effect have been used in other models (Lehman et al., 1975; Scavia,

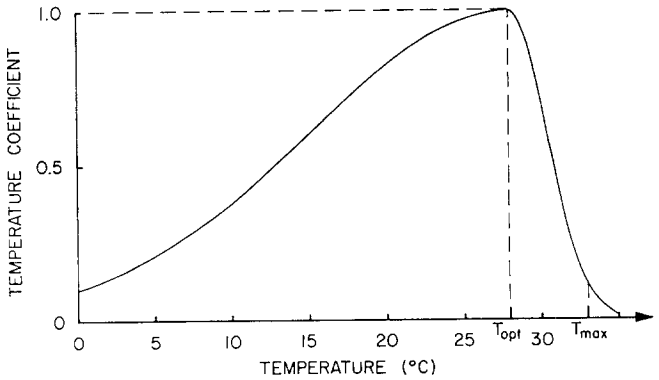

Fig. 5. Graphical representation of the temperature effect on growth for a species with optimum rate at 28° C (T_{opt}) and a 90% inhibiion at 33° C (T_{max}). The low-temperature 90% inhibition is taken to be at 0° C (T_{min}).

1980; Walters, 1980; Bierman, 1981). The temperature function should yield a maximum at the optimal temperature for nutrient saturated growth and decrease both above and below this level. A function of acceptable form without an excessive number of parameters is given by Lehman et al. (1975) as:

$$x = \exp\left(-2.3\left(\frac{T - T_{opt}}{T_{opt} - T_{min}}\right)^2\right) \qquad T < T_{opt} \tag{11}$$

$$x = \exp\left(-2.3\left(\frac{T - T_{opt}}{T_{max} - T_{opt}}\right)^2\right) \qquad T > T_{opt} \tag{12}$$

where x is fraction of reduced growth due to temperature ($0 \leqslant x \leqslant 1$); T_{opt} optimum temperature for nutrient saturated growth; T_{min} low temperature at which growth is reduced 90% from optimum (≈ 0° C); and T_{max} high temperature at which growth is reduced 90%.

A typical temperature curve is shown in Fig. 5. The function requires three reference temperatures: optimum, minimum, and maximum.

Phytoplankton populations are reduced by three processes: respiration, mortality, and settling. Each phytoplankton population is assigned a fixed settling velocity. The use of a single value is an approximation since the settling rates for an algal species may vary considerably with the physiological condition of the algae and increase with increasing stress on algal cells (Thomann et al., 1975). The stressed physiological condition is, however, most severe in the hypolimnion where little or no growth occurs.

Respiration is simulated in the level-2 and level-3 models by:

$$R = k_r \theta_r^{(T-20)}(\text{Chl.-}a) \tag{13}$$

where k_r is respiration rate constant (day^{-1}); θ_r temperature adjustment factor; T temperature in the layer (°C); and Chl.-a concentration of chlorophyll-a (mg l^{-1}).

The assumption is made that respiration is related only to the concentration of chlorophyll-a and temperature. Two values for k_r can be specified: one for the euphotic zone and one below the euphotic zone.

The mortality rate M in a phytoplankton population is modeled in the same manner as respiration:

$$M = k_m \theta_m^{T-20}(\text{Chl.-}a) \tag{14}$$

where k_m is mortality rate constant (day^{-1}); θ_m temperature adjustment factor; T temperature in the layer (°C); and Chl.-a concentration of chlorophyll-a (mg l^{-1}).

A schematic of the processes represented at each of the model levels is presented in Fig. 6. Differential equations for levels 2 and 3 of the phytoplankton model are given below.

- Level 2 (Michaelis–Menten growth function):

$$\frac{\partial\ \text{Chl.-}a}{\partial t} - \frac{1}{A}\frac{\partial}{\partial z}\left(AK_z \frac{\partial\ \text{Chl.-}a}{\partial z}\right) + \frac{V}{A}\frac{\partial(A\ \text{Chl.-}a)}{\partial z} + k_m\theta_m^{T-20}\text{Chl.-}a + k_r\theta_r^{T-20}\text{Chl.-}a - \mu_{max}\ f(T)\ \min\left[\frac{I\left(1+2\sqrt{K_1/K_2}\right)}{I+K_1+I^2/K_2} : \frac{P}{K_p+P}\right]\text{Chl.-}a = 0 \tag{15}$$

- Level 3 (Internal nutrient growth function):

$$\frac{\partial\ \text{Chl.-}a}{\partial t} - \frac{1}{A}\frac{\partial}{\partial z}\left(AK_z \frac{\partial\ \text{Chl.-}a}{\partial z}\right) + \frac{V}{A}\frac{\partial(A\ \text{Chl.-}a)}{\partial z} + k_m\theta_m^{T-20}\text{Chl.-}a + k_r\theta_r^{T-20}\text{Chl.-}a - \mu_{max}\ f(T)\ \min\left[\frac{I\left(1+2\sqrt{K_1/K_2}\right)}{I+K_1+I^2/K_2} : \frac{\text{NC} - \text{Chl.-}a(N_{min})}{\text{NC}} : \frac{\text{PC} - \text{Chl.-}a(P_{min})}{\text{PC}}\right]\text{Chl.-}a = 0 \tag{16}$$

where Chl.-a is chlorophyll-a concentration (mg l^{-1}); A area (m^2); K_z vertical eddy diffusivity ($m^2\ day^{-1}$); V settling velocity (m day^{-1}); k_m, k_r mortality and respiration rate (day^{-1}); θ temperature adjustment coefficient; T temperature (°C); μ_{max} maximum growth rate (day^{-1}); $f(T)$ temperature function for growth; I intensity of photosynthetically active radiation ($\mu E\ m^{-2}\ s^{-1}$); K_1, K_2 light limitation and inhibition coefficients;

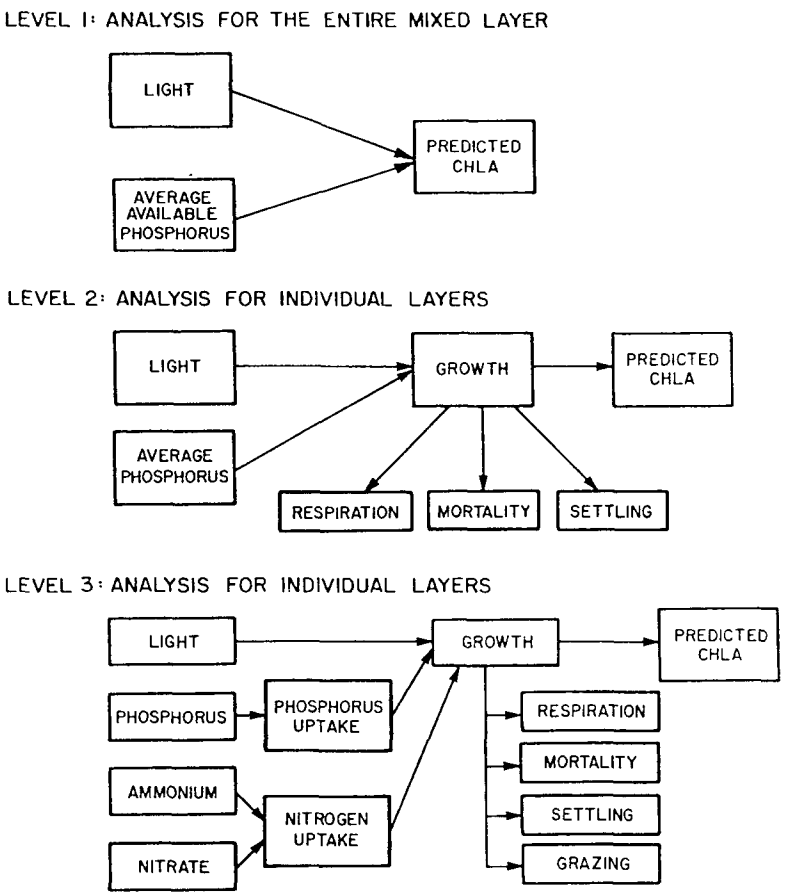

Fig. 6. Schematic illustration of the process affecting the predicted chlorophyll-*a* concentration in each level of the biological submodel.

respectively ($\mu E\ m^{-2}\ s^{-1}$); K_p half saturation constant for phosphorus-limited growth (mg l^{-1}); P available phosphorus concentration (mg l^{-1}); NC internal nitrogen concentration (mg l^{-1}); N_{min} minimum ratio of internal nitrogen to chlorophyll-*a*; and PC internal phosphorus concentration (mg l^{-1}); and P_{min} minimum internal ratio of internal phosphorus to chorophyll-*a*.

The three models of chlorophyll-*a* concentration differ in complexity and the number of calibration parameters. The first phytoplankton model requires the least amount of effort for calibration and requires the least computer time. The limitation of the first model is that phytoplankton growth is limited to the mixed layer and treated as constant throughout the mixed layer. Consequently, the first phytoplankton model would not be

recommended for evaluating lake restoration alternatives, but would be useful in the assessment of in-lake conditions when there are little in-lake data available and where time and cost constraints prohibit a more detailed study.

The second and third phytoplankton models are primarily to be used in the evaluation of lake restoration alternatives. The operation of each is similar, that is, they predict growth in each layer. The third model is slightly more complex than the second requiring more calibration coefficients and an extra state variable for the cellular nutrient concentration for each nutrient simulated. The difference in computer time between the second and third model is slight and, consequently, the decision to use one or the other is largely a matter of preference for Michaelis–Menten kinetics or cell quota kinetics.

Zooplankton

The treatment of zooplankton in the model differs from the treatment of all other variables. Zooplankton movement is not simply a combination of settling and diffusion, but the result of the individual mobility of the zooplankton. In many studies the effect of grazing and predation on a zooplankton population are related to the number of zooplankton rather than to the mass of zooplankton (see Kerfoot, 1980). Therefore a simple advection–diffusion model does not apply. The movement of zooplankton (especially large zooplankton) follows a pattern of vertical migration from deep water to the surface on the daily time scale. The retreat to deeper waters during the day provides zooplankton with a refuge from visual predators. At dusk, the zooplankton begin a vertical rise to the surface while grazing and by dawn they return to deeper layers. The 'day depth' of the zooplankton is fixed in the model as the depth at which the dissolved oxygen concentration is less than 0.5 mg l^{-1}. Predation on zooplankton may be taken to be a function of light availability at the day depth (Wright et al., 1980) or as a linear function of time.

The two periods of zooplankton activity are treated separately in the model. First, the day depth, light level at the day depth, and predation on zooplankton are computed. The respiratory and mortality losses contribute to the oxygen and nutrient budgets of the day depth layer in proportion to the length of the daylight period. Grazing at the day depth is not treated in the model. A second sequence of computations begins with the vertical rise in the evening. Grazing is assumed to occur in proportion to the chlorophyll-*a* concentration in a layer compared to the total chlorophyll-*a* concentration from the day depth to the surface. The effect of the proportion of chloro-

phyll in each layer is to simulate the time spent in each layer where the time (Δt) is given by:

$$\Delta t_i = \left(1 - \frac{\text{TD}}{24}\right)\left[\frac{\sum_{k=1}^{3} \text{Chl.-}a_{ik}}{\sum_{i=1}^{d}\sum_{k=1}^{3} \text{Chl.-}a_{ik}}\right] \tag{17}$$

where Δt_i is time increment for layer i (day); TD photoperiod (h); Chl.-a_{ik} chlorophyll-a concentration of phytoplankton group k in layer i; and d day depth layer

NUTRIENT MODEL

Typical eutrophication models treat phosphorus as the most significant nutrient, but many models also include nitrate–nitrite and ammonium for nitrogen limitation. In the MINLAKE model, phosphorus is the only limiting nutrient used in the level one and two models. Level 3 has nitrogen limitation as a user selected option.

Phosphorus. The first question to be answered in modeling phosphorus is which forms of phosphorus to model. Most phosphorus monitoring programs measure phosphorus as total phosphorus concentration. Approximately 5–50% of the total phosphorus is in a form that is readily used by phytoplankton. The readily accessible fraction is composed of orthophosphate and polyphosphate ions and is referred to as soluble reactive phosphorus (SRP) or dissolved reactive phosphorus (DRP). Another fraction of phosphorus exists in dissolved and particulate organic matter and is released as the organic matter decays. Phosphorus may also be adsorbed onto sediment particles or complexed with metal ions in solution and in the sediment. The present model treats only SRP as available phosphorus and, indirectly models organic phosphorus as detritus. The differential equation representing the phosphorus cycle is given below:

$$\begin{aligned}
&\frac{\partial P}{\partial t} - \frac{1}{A}\frac{\partial}{\partial z}\left(AK_z\frac{\partial P}{\partial z}\right) - \frac{S_{\text{p}}}{A}\left(\frac{\partial A}{\partial z}\right) - \sum_{n=1}^{3} k_{\text{r}_n}\theta_{\text{r}_n}^{T-20}\,\text{PC} \\
&\quad - \sum_{n=1}^{3} k_{\text{m}_n}\theta_{\text{m}_n}^{T-20}\left(\text{PC}_n - P_{\min_n}\text{Chl.-}a_n\right) \\
&\quad - k_2\theta_2^{T-20}\,\text{BOD YPBOD} \\
&\quad + \sum_{n=1}^{3} u_{\max_n}\theta_{u_n}^{T-20}\left(\frac{\text{Chl.-}a_n P_{\max_n} - \text{PC}_n}{\text{Chl.-}a_n\left(P_{\max_n} - P_{\min_n}\right)}\right)\left(\frac{P}{K_{\text{P}_n} + P}\right)\text{Chl.-}a_n = 0
\end{aligned} \tag{18}$$

where P is available phosphorus concentration (mg l^{-1}); A horizontal area (m^2); K_z vertical eddy diffusion coefficient (m^2 day^{-1}); S_p sediment phosphorus release rate (g m^{-2} day^{-1}); n algal group; k_r, k_m, k_2 reaction rate coefficients for respiration, mortality and organic decay, respectively (day^{-1}); θ temperature adjustment coefficient; PC internal phosphorus concentration (mg l^{-1}); P_{max} maximum internal nutrient ratio of mg phosphorus to mg chlorophyll; P_{min} minimum internal nutrient ratio of mg phosphorus to mg chlorophyll; Chl.-*a* chlorophyll concentration (mg l^{-1}); BOD concentration of BOD (mg l^{-1}); YPBOD ratio of mg phosphorus released to mg oxygen utilized in organic decay; u_{max} maximum specific uptake rate for phosphorus (mg P (mg Chl.-*a* day)$^{-1}$); and K_P half saturation constant for uptake of phosphorus (mg l^{-1}).

In the level-1 and level-2 models, phosphorus consumption is directly related to growth. The ratio of chlorophyll-*a* to phosphorus is treated as a constant yield ratio. Therefore, phosphorus consumption is given by:

$$\Delta P = \mu Y_{\text{PChl.-}a}\text{Chl.-}a \tag{19}$$

where μ is growth rate (day^{-1}); $Y_{\text{PChl.-}a}$ yield ratio of phosphorus to chlorophyll-*a*; and Chl.-*a* concentration of chlorophyll-*a* (mg l^{-1}).

The yield ratio is developed from a ratio of carbon to phosphorus (Stumm and Morgan, 1981) and the fixed chlorophyll-*a*/carbon ratio discussed earlier. The loss of phosphorus from algal cells is assumed to be more closely related to respiration than to either growth or uptake. Therefore, the respiration rate is used in much the same way as the growth rate, but to represent phosphorus release rather than consumption by algae. Mortality does not directly release phosphorus, but contributes to the detrital mass, from which the phosphorus is released through biological decay.

In the level-3 model, uptake of phosphorus by algae has a one-to-one correspondence with phosphorus depletion in the water. The internal phosphorus is independent of either the chlorophyll-*a* concentration or the carbon content and, therefore, no yield coefficient is required. Respiration rate is used as above to directly release internal phosphorus into the water. Mortality directly releases excess phosphorus, but the minimum chlorophyll-*a*/phosphorus ratio is used to apportion a fraction of the internal phosphorus to the detrital mass. This assumes that all excess phosphorus is stored as polyphosphates which go into solution as available phosphorus when the cells die (Jensen et al., 1976). Similarly, it is assumed that zooplankton grazing releases excess phosphorus to the water and retains the minimum level of phosphorus. Consequently, the phosphorus/mass ratio is assumed to be constant in both zooplankton and detritus. This assumption ignores any storage of phosphorus within zooplankton, but since the zooplankton biomass is small and the fraction of phosphorus fraction in

zooplankton is small, the total stored phosphorus within zooplankton should not introduce a serious error, but only result in slightly faster cycling of phosphorus.

The sediment of a lake contains a large store of phosphorus in organic matter, adsorbed to sediment, and complexed with metal ions. Under aerobic conditions the release of phosphorus from the sediments is generally at a rather slow and fairly constant rate. However, under anoxic conditions, the complexed portion can be rapidly mobilized causing a significant increase in the release rate. Presently, the release rate in MINLAKE is a constant, meaning that sediment phosphorus release is simulated as a zero-order process. If a different sediment release relationship is desired, phosphorus source terms can be added to the lake-specific subroutine.

Nitrogen. Nitrogen limitation is modeled only in the case of the first and second algal classes in model level-3. Nitrogen, like phosphorus, exists in many forms. However, uptake occurs almost exclusively from the nitrate–nitrite fractions and the ammonium fraction. There is also a preference in the uptake of ammonium over the uptake of nitrate–nitrite. In the present model, both nitrate–nitrite and ammonium are modeled separately. The differential equations for ammonium and nitrate–nitrite are present below:

$$\begin{aligned}
&\frac{\partial\ \mathrm{NH}}{\partial t} - \frac{1}{A}\frac{\partial}{\partial z}\left(AK_z\frac{\partial\ \mathrm{NH}}{\partial z}\right) - \sum_{n=1}^{3} k_{\mathrm{r}_n}\theta_{\mathrm{r}_n}^{T-20}\ \mathrm{NC}_n + k_{\mathrm{N}}\theta_{\mathrm{N}}^{T-20}\ \mathrm{NH} \\
&\quad - \frac{S_{\mathrm{N}}}{A}\left(\frac{\partial A}{\partial z}\right) \\
&\quad - k_2\theta_2^{T-20}\ \mathrm{BOD\ YNBOD} \\
&\quad + \sum_{n=1}^{3} u_{\mathrm{Nmax}_n}\theta_{u_{\mathrm{N}n}}^{T-20}\left(\frac{\text{Chl.-}a_n\ N_{\max_n} - \mathrm{NC}_n}{\text{Chl.-}a_n\left(N_{\max_n} - N_{\min_n}\right)}\right) \qquad (20) \\
&\qquad\qquad \left(\frac{\mathrm{NH}}{\mathrm{HSCNH}_n + \mathrm{NH}}\right)\left(\frac{\mathrm{NH} + \mathrm{NO}}{\mathrm{HSCN}_n + \mathrm{NH} + \mathrm{NO}}\right)\text{Chl.-}a_n \\
&\quad - \sum_{n=1}^{3} k_{\mathrm{m}_n}\theta_{\mathrm{m}_n}^{T-20}\left(\mathrm{NC}_n - \text{Chl.-}a_n\ N_{\min_n}\right) = 0
\end{aligned}$$

where NH is ammonium concentration (mg l^{-1}); A horizontal area (m^2); K_z vertical eddy diffusion coefficient (m^2 day^{-1}); n algal group; NC internal nitrogen concentration (mg l^{-1}); k_{r_n}, k_{N}, k_2, k_{m_n} rate coefficients for respiration, nitrification organic decay and mortality, respectively (day^{-1}); θ temperature adjustment coefficient; T temperature (°C); S_{N} sediment

release coefficient (g m^{-2} day^{-1}); BOD biochemical oxygen demand (BOD) (mg l^{-1}); YNBOD yield coefficient for mg N per mg BOD; u_{Nmax} maximum uptake rate (mg N (mg Chl.-*a* day)$^{-1}$); N_{max} maximum internal nutrient ratio of mg nitrogen per mg chlorophyll; N_{min} minimum internal nutrient ratio of mg nitrogen per mg chlorophyll; HSCNH half-saturation constant for preferential uptake of ammonium over nitrate (mg l^{-1}); HSCN half-saturation constant for total nitrogen uptake (mg l^{-1});

$$\frac{\partial\ \mathrm{NO}}{\partial t} - \frac{1}{A}\frac{\partial}{\partial z}\left(AK_z\frac{\partial\ \mathrm{NO}}{\partial z}\right) - k_N\theta_N^{T-20}\ \mathrm{NH} - \frac{S_{NO}}{A}\left(\frac{\partial A}{\partial z}\right) + \sum_{n=1}^{3} u_{\mathrm{Nmax}_n}\theta_{u_{Nn}}^{T-20}\left(1 - \frac{\mathrm{NH}}{\mathrm{HSCNH}_n + \mathrm{NH}}\right)\left(\frac{\text{Chl.-}a\ N_{\mathrm{min}_n} - \mathrm{NC}_n}{\text{Chl.-}a\left(N_{\mathrm{max}_n} - N_{\mathrm{min}_n}\right)}\right)\left(\frac{\mathrm{NH} + \mathrm{NO}}{\mathrm{HSCN}_n + \mathrm{NH} + \mathrm{NO}}\right)\text{Chl.-}a = 0 \quad (21)$$

where NO is nitrate–nitrite concentration (mg l^{-1}); A horizontal area (m^2); K_z vertical eddy diffusion coefficient (m^2 day^{-1}); z depth (m); k_N nitrification rate coefficient (day^{-1}); θ_N, θ_{u_N} temperature adjustment coefficients for nitrification and uptake, respectively; NH ammonium concentration (mg l^{-1}). S_{NO} sediment exchange coefficient (g m^{-2} day^{-1}); n algal group; u_{Nmax} maximum specific uptake rate (mg N (mg Chl.-*a* day)$^{-1}$), HSCNH half saturation coefficient for preferential uptake of ammonium over nitrate (mg l^{-1}); Chl.-*a* chlorophyll concentration (mg l^{-1}); N_{max} maximum internal nutrient ratio of mg nitrogen per mg chlorphyll, N_{min} minimum internal nutrient ratio of mg nitrogen per mg chlorophyll; and HSCN half saturation constant for nitrogen uptake (mg l^{-1})

Ammonium is modeled in a manner very similar to phosphorus. However, respiration, mortality, and grazing contribute to ammonium and only sediment exchange and nitrification contribute to the concentration of nitrate–nitrite.

The preference for ammonium over nitrate–nitrite in nitrogen uptake is modeled after Scavia (1980) as:

$$u' = u_{max}\left(\frac{\text{Chl.-}a\ N_{max} - N_c}{\text{Chl.-}a\ (N_{max} - N_{min})}\right)\left(\frac{\mathrm{NH} + \mathrm{NO}}{\mathrm{HSCN} + \mathrm{NH} + \mathrm{NO}}\right) \quad (22)$$

$$u_{NO} = u'\left(1 - \frac{\mathrm{NH}}{\mathrm{HSCNH} + \mathrm{NH}}\right) \qquad \text{nitrate–nitrite} \quad (23)$$

and

$$u_{NH} = u'\left(\frac{\mathrm{NH}}{\mathrm{HSCNH} + \mathrm{NH}}\right) \qquad \text{ammonium} \quad (24)$$

where u' is the internal and external nitrogen limited uptake rate (day^{-1}); Chl.-*a* concentration of chlorophyll-*a* (mg l^{-1}); N_{max} maximum

nitrogen/chlorophyll-*a* ratio; N_{min} minimum nitrogen/chlorophyll-*a* ratio; N_c internal nitrogen concentration (mg l^{-1}); NH ammonium concentration (mg l^{-1}); NO nitrate–nitrite concentration (mg l^{-1}); HSCH half saturation constant for nitrogen uptake (mg l^{-1}); HSCNH ammonium preference constant (mg l^{-1}); u_{NO} uptake rate of nitrate–nitrite (day^{-1}); u_{NH} uptake rate of ammonium (day^{-1}); and u_{max} maximum uptake rate of nitrogen (day^{-1}).

The ammonium preference ratio has the form of a Michaelis–Menten ratio and varies from 0 to 1. The preference constant is then defined as the ammonium concentration at which half of the nitrogen uptake is from ammonium and half from nitrate–nitrite.

Nitrification is treated as a one-step conversion given by (Scavia, 1980):

$$\Delta \text{ NO} = k_N \theta^{T-20} \text{ NH}$$

where Δ NO is increase in nitrite–nitrate (mg l^{-1}); K_N conversion rate coefficient (day^{-1}); θ temperature adjustment coefficient; and T temperature in a layer (°C).

DISSOLVED OXYGEN AND DETRITUS (BOD)

The conversion of dissolved oxygen is seldom a variable in entrophication models. Oxygen does not directly affect phytoplankton. However, dissolved oxygen directly effects biological decay processes, sediment nutrient release rates, and the vertical migration of zooplankton. It is included as a variable in the present model to aid in simulating the movement of large zooplankton and to simulate lake restoration techniques that affect dissolved oxygen, such as hypolimetric aeration.

In the model, dissolved oxygen is provided from two sources. First, at the lake surface, diffusion of oxygen occurs to attain an equilibrium between the dissolved oxygen in the air and in the water. Secondly, the photosynthetic process produces oxygen. The surface diffusion is modeled using the saturation deficit given by:

$$\Delta O = K_o(O_{sat} - O_1) \tag{25}$$

where ΔO is change in dissolved oxygen (mg l^{-1} day^{-1}); K_o exchange coefficient (day^{-1}); O_{sat} saturated oxygen concentration (mg l^{-1}); and O_1 oxygen concentration in the surface (first) water layer (mg l^{-1}).

The saturated oxygen concentration O_{sat} (mg l^{-1}) is temperature-dependent and given by:

$$O_{sat} = 14.652 - 0.41022T + 7.99 \times 10^{-3}T^2 - 7.7774 \times 10^{-5}T^3$$

where T is surface temperature (°C).

The oxygen exchange coefficient is not a constant and varies widely (Mattingly, 1977). Many relationships have been developed to estimate the oxygen exchange coefficient (Yu et al., 1977). In the present model, the

oxygen exchange coefficient is predicted from:

$$K_O = \frac{0.641 + 0.0256W^2}{d_1} \tag{26}$$

where K_O is exchange coefficient; W wind speed (MPH $\approx$ 1.609 km $h^{-1} \approx$ 0.447 m s^{-1}); and d_1 thickness of first layer (m).

Oxygen is depleted from a layer by the combined actions of respiration, sediment uptake, nitrification, and organic decay of detritus (BOD). Respiration is treated in the same manner as stated previously by equation (13), but with a different yield coefficient. Likewise, sediment uptake of dissolved oxygen is treated in the same manner as sediment exchange of phosphorus, but with different rate coefficients.

The microbial decay of organic matter follows the same pattern as nitrification, but is a function of the detrital mass expressed in oxygen equivalents. The mortality of cells and a fraction of the grazed phytoplankton are converted from chlorophyll-*a* concentrations to oxygen equivalents using a constant carbon–chlorophyll-*a* ratio and stoichiometric relationships (Stumm and Morgan, 1981). The result is a one-to-one correspondence between the decay of detritus and the utilization of oxygen:

$$\Delta O = \Delta \text{ BOD} = k_2 \theta^{T-20} \text{ BOD} \tag{27}$$

where ΔO is decrease in oxygen (mg l^{-1} day^{-1}); Δ BOD decrease in detritus as oxygen equivalents (mg l^{-1}); k_2 first-order decay coefficient (day^{-1}); θ temperature adjustment coefficient; T temperature (°C); and BOD detritus as oxygen equivalents (mg l^{-1}).

The linked BOD and dissolved oxygen equations are presented below:

- BOD

$$\frac{\partial \text{ BOD}}{\partial t} - \frac{1}{A}\frac{\partial}{\partial z}\left(AK_z \frac{\partial \text{ BOD}}{\partial z}\right) + \frac{V}{A}\frac{\partial (A \text{ BOD})}{\partial z} - \frac{1}{\text{YPBOD}} \sum_{n=1}^{3} \left(k_{\text{m}_n} \theta_{\text{m}_n}^{T-20} \text{ Chl.-}a_n \, P_{\min_n}\right) + k_2 \theta_{\text{BOD}}^{T-20} \text{ BOD} = 0 \tag{28}$$

- Dissolved oxygen

$$\frac{\partial \text{ DO}}{\partial t} - \frac{1}{A}\frac{\partial}{\partial z}\left(AK_z \frac{\partial \text{ DO}}{\partial z}\right) + \frac{1}{\text{YCHO2}} \sum_{n=1}^{3} \left(k_{\text{r}_n} \theta_{\text{r}_n}^{T-20} - \mu_{\max} \text{ f}(T) \min[L, P, N](\text{Chl.-}a_n)\right) + k_2 \theta_{BOD}^{T-20} \text{ BOD} + \frac{S_b}{A}\frac{\partial A}{\partial z} + \frac{1}{\text{YNHO2}} k_{\text{NH}} \theta_{\text{NH}}^{T-20} \text{ NH} - K_O(O_{\text{sat}} - \text{DO})_{\text{surface}} = 0 \tag{29}$$

where BOD is biochemical oxygen demand (mg l^{-1}); A horizontal area (m^2); K_z vertical eddy diffusivity (m^2 day^{-1}); V settling velocity (m day^{-1}); n algal group; YPBOD ratio of mg phosphorus to mg BOD in detritus; k_m, k_r mortality and respiration rate coefficients, respectively (day^{-1}); θ temperature adjustment coefficients; T temperature (°C); $P_{\min_n}$ minimum internal nutrient ratio of mg phosphorus to mg chlorophyll-a for algal group n; k_2 organic decomposition rate (day^{-1}); DO dissolved oxygen concentration (mg l^{-1}); YCHO2 ratio of mg chlorophyll per mg oxygen utilized in respiration and photosynthesis; μ_{max} maximum growth rate (day^{-1}); f(T) temperature function for growth; L light-limited growth ratio; P phosphorus-limited growth ratio; N nitrogen-limited growth ratio; S_b rate of oxygen utilized at the water sediment interface (g m^{-2} day^{-1}); YNHO2 ratio of mg ammonium

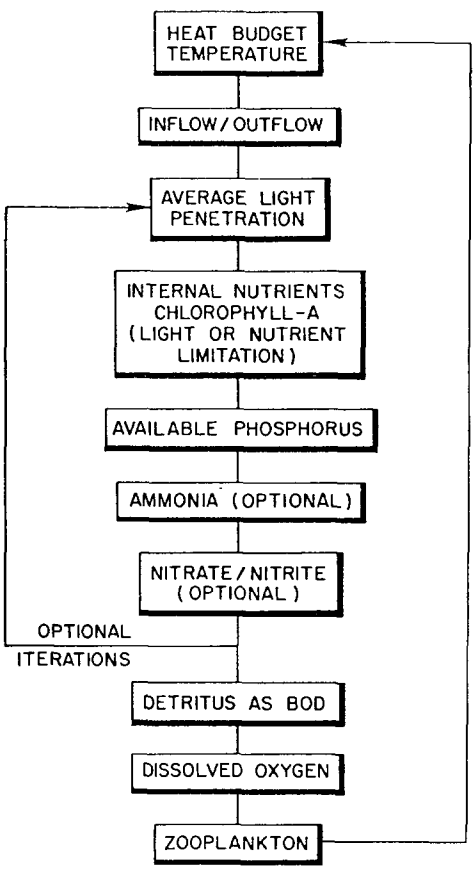

Fig. 7. Flow chart illustrating the state variables simulated and the sequential order of the solution procedure.

consumed per mg oxygen utilized in nitrification; K_{NH} nitrification rate coefficient (day^{-1}); O_{sat} saturated oxygen concentration ($mg\ l^{-1}$); and K_O surface oxygen exchange rate (day^{-1}).

METHOD OF SOLUTION

In a lake, the processes of heat transfer, wind mixing, inflow/outflow, growth, etc., occur simultaneously. In simulating the processes, the model must either use a single large, sparse matrix solution for all variables simultaneously or the processes must be treated in a sequential manner.

The integral energy heat budget model as formulated by Ford and Stefan (1980) uses a sequential treatment of heat flux in, heat flux out, and wind mixing. This same sequential formulation was then applied to all other variables. The progression of processes is from the physical processes of heat flux, wind mixing, inflow/outflow, and conservative, suspended and dissolved substances to the biological processes of nutrient uptake, growth, nutrient depletion and oxygen depletion.

The purpose of the progression order is to treat first those processes that have a greater effect on other processes. For example, the temperature profile, which affects both physical mixing and reaction rates, is predicted first and the nutrient/growth kinetics, which do not significantly affect temperature, are predicted later in the progression. Figure 7 illustrates the order in which the solution occurs.

MODEL OPERATION

The main design criteria for the operation of the model are accuracy, economy, and ease of operation. For ease of operation, it was decided to make the model interactive with the user and to provide the option of graphical output at intermediate times in the simulation. For ease of calibration, the model provides an option to re-initialize the simulation and make changes to selected calibration parameters. The model then runs in a continuous mode with the operator viewing graphical results, deciding on modifications to parameters and restarting the simulation as needed. The continuous interactive mode of operation would be too costly on a main frame computer. Consequently, the economic constraint was satisfied by using IBM-AT and IBM-AT compatible microcomputers. The microcomputers were found to be adequate in speed, taking approximately 3 min to simulate a 6-month growing season and do not have the cost disadvantage of a mainframe computer running interactively.

MODEL OUTPUT

The model generates both tabular and graphical output. The tabular output lists the profiles of all state variables as well as meteorological and heat budget information, inflow and outflow quantities, and mixed layer and secchi depths. Graphical output is available in one of two formats. The user may select profile plots at specified days (such as days for which field data are available) and time series plots for specified depths. Both profile and time series plots may be viewed during the operation of the model and hardcopy output may be selected for any graph. The data for the time series plots are stored in an external file and may be used to produce seasonal time series such as isothermal contours and other isometric diagrams. An example of model application can be found in Riley et al. (1987).

CONCLUSIONS

Most lake simulation models fall into one of the following four categories: steady-state (non-dynamic) models (Dillon and Rigler, 1975; Vollenweider, 1975); time-dynamic well mixed models (Jørgensen, 1976; Jørgensen et al., 1978); depth and time-dynamic models (Walters, 1980; Scavia, 1980); and multi-dimensional space and time-dynamic models (Bierman, 1981). Most dynamic models have drawbacks in terms of applicability to lakes of different physical characteristics and ease of use. Most of the existing models are not specifically designed as simulation tools for the evaluation of multiple and varied lake restoration techniques. The MINLAKE model is designed to fill this need. Designed for small lakes, on the order of tens of kilometers square or less, either deep or shallow, the model retains the depth and time dynamics of more complex models, but adds the capability of being a generalized management tool. The model balances the space and time dynamics with the requirements for computational cost, accuracy and stability.

To satisfy the cost requirement, the program has been developed for IBM compatible microcomputers. For maximum speed, an IBM-AT or faster compatible is preferred with a run time on the order of 3 min for a simulation of a 5-month summer season.

A wide range of lake management techniques have been reviewed and preliminary methods have been identified for incorporating management practices into the model (Hanson et al., 1987).

The MINLAKE model offers a unique collection of features in a lake simulation program. The model is structured to use the physical characteristics specific to a study lake in simulating the dynamic interactions of the variables with depth on a daily basis. The model provides a versatile and

flexible management tool for the evaluation of lake restoration alternatives by limnologists, engineers, and lake management agencies.

ACKNOWLEDGMENT

Material presented in this paper is based in part on work done under a grant from the Legislative Commission on Minnesota Resources, St. Paul, MN, U.S.A.

REFERENCES

Bannister, T.T., 1974. A general theory of steady-state phytoplankton growth in a nutrient saturated mixed layer. Limnol. Oceanogr., 19: 13–20.

Bierman, V.J., Jr. and Dolan, D.M., 1981. Modelling phytoplankton-nutrient dynamics in Saginaw Bay. J. Great Lake Res., 7: 409–439.

Cardoni, J. and Stefan, H.G., 1981. A model for light and temperature limited primary productivity in Lake Chicot. Ext. Memo, 176, St. Anthony Falls Hydraulic Laboratory, University of Minnesota, Minneapolis, MN, 96 pp.

Cochrane, K.L., Ashton, P.J., Jarvis, A.C., Twinch, A.J. and Zohary, T., 1987. An ecosystem model of phosphorus cycling in a warm monomictic, hypertrophic impoundment. Ecol. Modelling, 37: 207–233.

Combs, W.S., 1977. The measurement and prediction of irradiance available for photosynthesis by phytoplankton in lakes. Ph.D. thesis, University of Minnesota, Minneapolis, MN, 225 pp.

De Groot, W.T., 1983. Modelling the multiple nutrient limitation of algal growth. Ecol. Modelling, 18: 99–119.

Dhamotharan, S., Gulliver, J. and Stefan, H., 1981. Unsteady one-dimensional settling of suspended sediment. Water Resour. Res., 17: 1125–1132.

Dillon, P.J. and Rigler, F.H., 1975. A test of a simple nutrient budget model predicting the phosphorus concentration in lake water. J. Fish. Res. Board Can., 32: 1519–1531.

DiToro, D.M., 1980. Applicability of cellular equilibrium and Monod theory to phytoplankton growth kinetics. Ecol. Modelling, 8: 201–208.

DiToro, D.M. and Connolly, J.P., 1980. Mathematical models of water quality in large lakes, II. EPA-600/3-80-65, Environmental Protection Agency, Grosse Isle, MI, 231 pp.

Ford, D.E. and Stefan, H., 1980. Thermal prediction using integral energy model. J. Hydraul. Div. ASCE, 106 (HY1): 39–55.

Forsberg, B.R. and Shapiro, J., 1981. The effects of artificial destratification on algal populations. In: H.G. Stefan (Editor), Proc. Symp. Surface Water Impoundments, June 1980, Minneapolis, MN. American Society of Civil Engineers, New York, pp. 851–864.

Gibbs, R.J., Mathews, M.D. and Link, D.A., 1971. The relationship between sphere size and settling velocity. J. Sediment. Petrol., 41: 7–18.

Gulliver, J.S. and Stefan, H.G., 1982. Lake phytoplankton model with destratification. J. Environ. Eng. Div. ASCE, 108 (EE5): 864–882.

Hanson, M.J. and Stefan, H.G., 1985. Shallow lake water quality improvement by dredging. In: Lake and Reservoir Management: Practical Applications. Proc. 4th Annu. Conf. Lake and Watershed Management, October 1984, North American Lake Management Society, ISSN 0743-8141, Washington, DC, pp. 162–171.

Hanson, M.J., Riley, M.J. and Stefan, H.G., 1987. An introduction to mathematical modeling of lake processes for management decisions. Proj. Rep. 249, St. Anthony Falls Hydraulic Laboratory, University of Minnesota, Minneapolis, MN, 105 pp.

Jassby, A. and Powell, T., 1975. Vertical patterns of eddy diffusion during stratification in Castle Lake, California. Limnol. Oceanogr. 20: 530–543.

Jensen, T.E., Sicko-Groad, L. and Lehman, H.H., 1976. Aspects of phosphate utilization by blue-green algae. EPA-600/3-76-103, Environmental Protection Agency, Corvallis, OR, 122 pp.

Jørgensen, S.E., 1976. A eutrophication model for a lake. Ecol. Modelling, 2: 147–165.

Jørgensen, S.E., Mejer, H. and Friis, M., 1978. Examination of a lake model. Ecol. Modelling, 4: 253–278.

Kerfoot, W.C. (Editor), 1980. Evolution and Ecology of Zooplankton Communities. University Press of New England, Hanover, NH, 793 pp.

Lehman, J.T., Botkin, D.B. and Likens, G.E., 1975. The assumptions and rationales of a computer model of phytoplankton population dynamics. Limnol. Oceanogr. 20: 343–364.

Matsuoka, Y., Goda, T. and Naito, M., 1986. A eutrophication model of Lake Kasumigaura. Ecol. Modelling, 31: 201–219.

Mattingly, G.E., 1977. Experimental study of wind effects on reaeration. J. Hydraul. Div. ASCE, 103 (HY3): 311–323.

Megard, R.O., Combs, W.S., Jr., Smith, P.D. and Knoll, H.S., 1979. Attenuating light and daily integral rates of photosynthesis attained by planktonic algae. Limnol. Oceanogr., 24: 1038–1050.

Megard, R.O., Tonkyn, D.W. and Senft, W.H., III, 1984. Kinetics of oxygenic photosynthesis in planktonic algae. J. Plankton Res., 6: 325–337.

Monod, J., 1949. The growth of bacterial cultures. Annu. Rev. Microbiol., 3: 371–394.

Mortimer, 1942. The exchange of dissolved substances between mud and water in lakes. J. Ecol., 30: 147–201.

Patankar, S.V., 1979. Numerical Heat Transfer and Fluid Flow. McGraw-Hill, New York, 179 pp.

Riley, M.J. and Stefan, H.G., 1986. Dynamic Lake Water Quality Modeling. Proc. 1986 Eastern Simulation Conf., Society for Computer Simulation, San Diego, CA.

Riley, M.J., Stefan, H.G., Shapiro, J. and Wright, D., 1988. Predictability of biomanipulation of Round Lake, Minnesota. Water Res. (submitted).

Scavia, D., 1980. An ecological model of Lake Ontario. Ecol. Modelling, 8: 49–78.

Schlesinger, D.A. and Shuter, B.J., 1981. Patterns of growth and cell computation of freshwater algae in light-limited continuous cultures. J. Phycol., 17: 250–256.

Stefan, H.G., Cardoni, J.J. and Fu, A.Y., 1982. RESQUAL II; a dynamic water quality simulation program for a stratified shallow lake or reservoir: application to Lake Chicot, Arkansas. Proj. Rep. 209, St. Anthony Falls Hydraulic Laboratory, University of Minnesota, Minneapolis, MN, 133 pp.

Stumm, W. and Morgan, J.J., 1981. Aquatic Chemistry (2nd Edition). Wiley-Interscience, New York, 780 pp.

Thomann, R.V., DiToro, D.M., Winfield, R.P. and O'Connor, D.J., 1975. Mathematical modeling of phytoplankton in Lake Ontario, 1. EPA 600/3-75-005, U.S. Environmental Protection Agency, Corvallis, OR, 77 pp.

Vollenweider, R.A., 1975. Input–output models with special reference to the phosphorus loading concept in limnology. Schweiz. Z. Hydrol., 37: 53–84.

Walker, W.W., Jr., 1986. Models and software for reservoir eutrophication assessment. In: Proc. Int. Symp. Applied Lake and Watershed Management, North American Lake Management Society, November 1985.

Walters, R.A., 1980. A time- and depth-dependent model for physical, chemical, and biological cycles in temperate lakes. Ecol. Modelling, 8: 79–96.

Wright, D., O'Brien, W.J. and Vinyard, G.L., 1980. Adaptive value of vertical migration: simulation model argument for the predation hypothesis. In: W.C. Kerfoot (Editor), Evolution and Ecology of Zooplankton Communities. University Press of New England, Hanover, NH, pp. 138–147.

Yu, S.L., Tuffey, T.J. and Lee, D.S., 1977. Atmospheric reaeration in a lake. Water Resources Research Institute, Rutgers University, New Brunswick, NJ, 50 pp.